

Experimental Studies on Abrasive Water Jet Cutting of Nano SiC Particles Filled Hybrid Basalt-Glass Fibre-Reinforced Epoxy Composites

S. Vijayabhaskar^{1,#}, T. Rajmohan^{1,*}, D. Vijayan^{1,†} and K. Palanikumar^{2,&}

¹Department of Mechanical Engineering, Sri Chandrasekharendra Saraswathi Viswa Maha Vidyalyaya, Enathur, Kanchipuram, 631561, India

²Department of Mechanical Engineering, Sri Sairam Institute of Technology, Chennai - 600044, India

Abstract: Abrasive water jet machining (AWJM) is extensively beneficial in machining materials that are hard to cut. This investigation deals with AWJM of Nano SiC filled Epoxy reinforced with basalt-glass fiber hybrid composite. The composite is prepared by compression moulding technique. Experimental trails are performed to evaluate the impact of every process parameter on the responses i.e., surface roughness (Ra) and Material Removal Rate (MRR). The experiments are conducted by changing the standoff distance (SD), traverse speed (TS) and water pressure. The performance of the conducted experiment is analysed using a Swarm intelligence algorithm. Surface roughness and MRR are maximized by using the combination of optimum process parameter levels of 9.72 mm/min speed, 5.78 mm stand-off distance and 553 MPa jet pressure. Scanning Electron Microscopic (SEM) images are employed in detecting the morphology of machined surface and confirmed the presence of voids and fibre pull-out.

Keywords: AWJ, Basalt-glass, MRR, Surface roughness, Nano SiC, Swarm intelligence algorithm, SEM.

1. INTRODUCTION

During recent times, the composites reinforced with natural fibre fashioned an excessive attention among researchers near technological developments. High-tech fibre acts as a vital basis in aiding the progress of advanced and modern technology industries and also obtained excessive significance in nation building. Recently, the demand for the products of such fibre composite materials is increasing rapidly at a mean yearly progress of 30% [1]. Among different fibre available, the basalt fibre is a novel material that is extensively utilized in defence and nonmilitary applications like agriculture, architecture, electronics, medicine, chemical industry, aerospace, etc., Basalt fibre is considered as one of the present-day materials obtained by melting basalt rock at 1450-1500°C via Platinum-rhodium alloy bushing. The studies on basalt fibre are in initial phases until now, thus investigations on the basalt fibre composite's performances has become academically as well as tactically important. Further treatment is necessary when the composite is used for specific applications [2].

Epoxy is a versatile thermosetting polymer with a wide range of applications. It is known for its excellent mechanical properties, electrical insulation, chemical/corrosion resistance, low curing shrinkage and high adhesion strength. Epoxy is used in a variety of industries, including fiber-reinforced composites, construction, adhesives, electronic materials and coatings [3]. Polymer matrix composites lack a

crystalline arrangement and do not exhibit plastic deformation capacity. Their composition is non-uniform and frequently demonstrates orthotropic characteristics [4]. Natural fiber-reinforced polymeric composites have been used as a cost-effective and sustainable alternative to fiber-reinforced composites made from petrochemical derivatives [5].

Currently, cutting-edge manufacturing methods are generally employed in resolving numerous problems in fabrication processes which comprise machining tough materials, making of contours with complicated geometry and improved surface topographies. Amidst several leading manufacturing methods, abrasive water jet (AWJ) machining gained additional consideration among investigators and professional engineers in production sector owing to its competence of wide processes along with outstanding characteristic of the state-of-the-art attained through this method significantly prominent than the rest, in accordance with the past investigators [6].

The process of erosion removes material in AWJ machining in which suspension of tough abrasive particles in the stream of water jet at elevated velocity that result in increased abrasive particle kinetic energy and acceleration striking the desired material [7]. The traditional methods are replaced by non-conventional energy sources with the advancements in technologies. For instance, abrasive particles in water are used as the source in AWJM for cutting composite materials [8].

The erosion plays a vital task in improving the cutting performance of AWJM. Deformation wear and cutting wear are the major mechanisms through which erosion occurs [9, 10]. The impact of abrasive particles

*Address correspondence to this author at the Department of Mechanical Engineering, Sri Chandrasekharendra Saraswathi Viswa Maha Vidyalyaya, Enathur, Kanchipuram, 631561, India; E-mail: rajmohanscsmv@yahoo.com
Co-Authors Email ID: #mailvijayabhaskar@gmail.com,
†vijaiand2012@gmail.com, &palanikumar_k@yahoo.com

produces contact stresses resulting in chipping and crack propagation through which material removal occurs in brittle erosion process [11]. Apart from work material erosion mechanism, depth of penetration is a significant output parameter for both AWJM performances and work material. Earlier investigators employed work materials in trapezoidal forms with varying thickness to examine AWJM for depth of penetration [12].

Hlaváč (2009) [13] studied the characteristics of AWJM machined surfaces in various types of materials like quartz, glass, steel, sand stone, limestone, marble, granite, etc., Srinivas and Babu (2011) [14] established the factors such as traverse rate and water jet pressure contribute in achieving high depth of penetration in Al metal matrix composites reinforced with SiC particles. Wang and Wong (1999) [15] stated that during AWJM of polymer matrix composites, more desirable machining performance is obtained at 80° jet impingement angle. Azmir and Ahsan (2009) [16] optimized the process parameters of AWJM such as taper ratio and surface roughness during machining of polymer composites reinforced with aramid fibre by developing a mathematical model employing multi linear regression analysis through the single response mode. The most dominating factor for these process parameters is found to be traverse rate as indicated by the ANOVA test result. Amuthakkannan *et al.*, (2021) [17] employed grey relational analysis while machining the composites reinforced with basalt fibre through AWJM considering the following process parameters such as water pressure, stand-off distance and nozzle travel speed.

Careful review of the literature reveals that only a very few researches have been carried out in the area of AWJM on hybrid epoxy composites reinforced with basalt-glass fibre filled with SiC nanoparticles. Hence,

this investigation examines the performance and effect of AWJM input parameters like standoff distance, traverse speed (TS) and water pressure on MRR and surface roughness. The appropriate process parameters are recommended in accomplishing optimal output and the morphology of the machined surface is detected using SEM images. The performance of the conducted experiment is analysed using a swarm intelligence algorithm. Since, several latest algorithms are devised to solve combinations and numerical optimization issues. The mentioned algorithms are certainly categorized into various types, according to the standards followed, namely population-based, repetitive base, probability theory, and determination theory [18]. Algorithms that try to improve them using a series of solutions are called the population based, but those that use multiple repetitions to approach the required solution are called iterative algorithms. If the algorithm adopts a stochastic rule to improve the solution, it is called a probabilistic or stochastic. Another classification can be performed according to the nature. This type of classification distinguishes two groups of important algorithms mainly through evolutionary algorithms (EAs) and swarm-intelligence based algorithmic [19]. Swarm intelligence algorithm is most popular algorithm used in minimization problems. This attained a huge consideration from researchers in numerous research fields and employed in several real-life problems [20]. Hence, the present investigation has been organised by employing swarm intelligence algorithm to estimate the optimum values of the AWJM cutting parameters.

2. EXPERIMENTAL

2.1. Materials and Method

The epoxy resin, glass fibers, and Basalt fibers sourced from ECO Craft in Hosur and Suntech Fibres



Sample A



Sample B

Figure 1: Prepared samples.

Table 1: Physical Properties of Resin and Fibers

Physical properties	Epoxy Resin	Basalt Fiber	Glass Fiber
Tensile Strength (Mpa)	90~120	3100~4840	2000~3500
Modulus of Elasticity (GPa)	3.1 ~ 3.8	85~95	70
Density (g/cm ³)	1.2 ~ 1.3	2.8	2.5
Elongation at Break (%)	4	3.15	2.5
Viscosity at 25 °C (kg/m s)	0.25–0.75	-	-
Glass transition temperatures	150 to 220 °C	-	-

Table 2: Composition of Prepared Composites

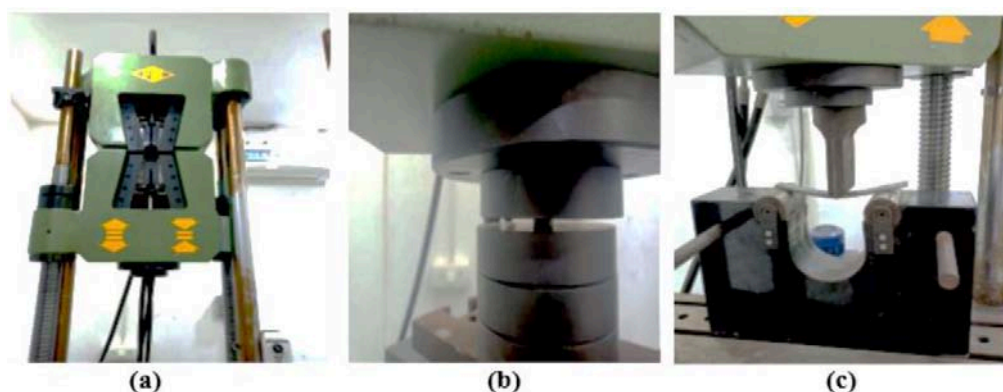
Sample Name	Number of layers of basalt fabric	Number of layers of glass fabric	Wt. % Nano SiC	Wt. % glass fibre	Wt.% basalt fibre	Wt.% Epoxy Resin
A	4	3	0	20	20	60
B	4	3	1	20	20	60

in Chennai, India and Nano SiC particles obtained from M/s US Research Nano Materials Inc in the USA were used for the fabrication. The epoxy resin was effectively mixed with 0% and 1% weight percent of Nano SiC particles using an ultrasonic probe sonicator, ensuring a homogeneous dispersion without any agglomeration (Mohan and Rajmohan, 2017). Table 1 presents the properties of epoxy resin and fibers used in the fabrication. The modified epoxy and hardener were blended in 10:1 ratio. The composite material was fabricated using compression moulding technique by arranging the glass fibers successively, while the Basalt fibers were positioned at both the bottom and top layers. A temperature of 50 °C and a pressure of 100 bar were the process parameters for the

compression moulding process. To ensure proper curing, the laminates were kept inside the compression moulding machine for a duration of 4 hours. Table 2 presents the composition of the fabricated composites.

The samples were subjected to a tensile test following ASTM D638 standard on universal testing machine with a capacity of 100 KN and strain rate of 0.001 s/mm as shown in Figure 2a. The tests were conducted at various tensile rates, varying from 1 to 500 mm/min, till the specimen reached failure, either by yielding or breaking. The test results are presented in Table 3.

The compression tests on the prepared samples were carried out based on ASTM D695 standard. The

**Figure 2: (a) Tensile Testing (b) Compressive Testing (c) Flexural Testing.****Table 3: Mechanical Properties of Prepared Samples**

S. No	Sample	Tensile Strength MPa	Compressive Strength MPa	Flexural Strength MPa
1	Sample A	74.63	170.74	138.79
2	Sample B	215.9	327.69	238.64

samples for the test were prepared into blocks with the dimensions of 10 x 10 x 4 mm. The compression testing machine applies a constant rate of compression to the test samples by exerting pressure between the plates, as depicted in Figure 2b. and the force on the samples was applied at a speed of 1.3 mm/min. The maximum compressive strength is noted and the average value of three samples was considered. Table 3 displays the results obtained from the tests.

The flexural tests were performed adopting ASTM D790 standards. These standards outline the procedure for 3-point flexure tests on rigid and semi-rigid plastics, along with long-fiber reinforced composites, as shown in Figure 2c. Parameters such as the maximum deflection, loading speed and support span were taken into account, considering the thickness of the specimen. Table 3 represents the outcomes of the tests.

Izod Impact Testing (Notched Izod) following ASTM D256 standard was carried out on the prepared samples to understand notch sensitivity. Notched Izod Impact testing as shown in the Figure 3 reveals a single-point test utilized to assess a material's resistance to impact caused by a swinging pendulum. Table 4 displays the results and average of three measurements were considered.



Figure 3: Izod Impact Testing.

Table 4: Impact Strength of Prepared Samples

S. No	Sample	Impact Strength J/m ²
1	Sample A	8.8
		8.8
		8.33
2	Sample B	14.55
		15.23
		15.55

In the process of Abrasive Water Jet Machining, a high-speed and high-force mixture of water and abrasive is focused on the surface of the workpiece, where it impinges and causes erosion. This erosion occurs due to the conversion of kinetic energy from the water and abrasive into pressure energy, resulting in the wearing away of the work material at the striking zone [22]. In this erosion process, a crucial role is being played by the kinetic energy of the abrasive particles. The abrasive particles are carried by high-pressurized water, which acts as the carrier medium. The schematic representation of the material erosion mechanism in the AWJM process is presented in Figure 4. The machine setup comprises various components, including working chamber, XY motion controller, mixture nozzle, abrasive tank, metering valve, intensifier pump, a booster pump and more.

The machine tool used for present work is manufactured by Water jet Germany Pvt. Ltd. and model number is S3015, a CNC machine.

2.2. Experimental Design

The control parameters in this study include jet pressure, wt % of nano SiC, standoff distance and traverse speed. Material removal rate (MRR) and surface roughness (SR) were measured as objective functions for optimization purposes and the development of a predictive model. Response Surface Methodology (RSM) based D-Optimal design was employed to plan for the experiments in which four control parameters were varied over three levels contributing to 24 experimental runs. The results of the experiment are presented in Table 5.

2.3. Swarm Intelligence Algorithm

Karaboga and Basturk (2008) [23] proposed a swarm intelligence algorithm inspired by the foraging behavior of bees. This algorithm was specifically designed for addressing numerical optimization problems. Swarm intelligence algorithm is an intelligent bee colony algorithm that simulates bees searching for nectar. These algorithms have several advantages, including high-quality solutions, excellent local search capabilities, and an updated mechanism for solving problems [24, 25]. In addition to improving local search capabilities, this also increases swarm stochasticity. As a swarm-based optimization method, it is currently one of the most popular. Based on the quantity and quality of nectar, a food source's quality (fitness) is determined biologically. And moreover, the most important feature of the artificial bee colony is that only one objective function should be given without too many requirements and additional external data.

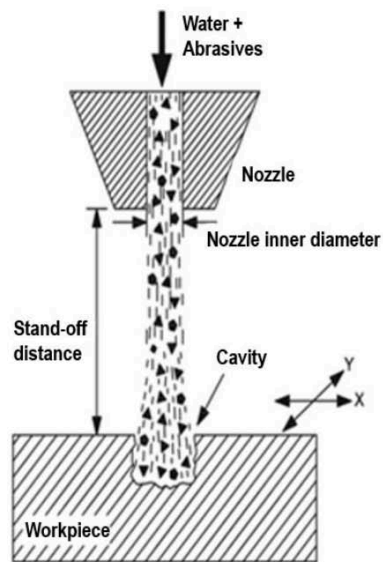


Figure 4: Abrasive Water Jet Machine.

Table 5: Experimental Results

S. No	Jet Pressure MPa	Stand-off Distance mm	Speed mm/min	Sample	SR μm	MRR mm^3/sec
1	200	15	10	B	1.884	0.92
2	400	3	2	A	1.489	0.18
3	400	12	8	B	1.825	0.75
4	200	9	6	B	1.633	0.54
5	200	15	2	A	1.591	0.14
6	200	15	2	A	1.624	0.14
7	200	3	2	B	1.451	0.12
8	600	15	2	A	1.483	0.2
9	600	9	6	A	1.832	0.57
10	200	3	10	A	2.219	0.72
11	300	9	6	A	1.716	0.5
12	400	3	10	B	1.907	0.98
13	400	15	10	A	2.108	0.87
14	600	15	6	B	1.57	0.58
15	600	3	10	A	2.256	1
16	400	15	2	B	1.515	0.22
17	600	15	6	B	1.694	0.68
18	600	3	2	B	1.41	0.34
19	400	6	4	B	1.59	0.4
20	200	3	2	A	1.495	0.12
21	600	9	10	B	1.977	0.98
22	200	3	10	A	1.951	0.74
23	600	9	10	B	1.967	1.05
24	400	15	10	A	1.924	0.9

In the algorithm, an analogy is made between bees and the optimization process. with certain assumptions, each nectar source is assigned to a unique bee [26].

The number of nectar sources corresponds to the number of involved bees in the algorithm. The sources represent possible decisions for the food problem

being solved, and the sum of nutrients associated with each source indicates the decision quality. The algorithm consists of various bee groups including: workers (researchers), observers, and boy scouts. The number of worker bees and observer bees is equal. When a nectar source is exhausted, the worker bee is reassigned to search for a new source, becoming a carrier bee. A mathematical expression that ranges between 0 and 1, known as the correspondence magnitude is used to evaluate the quality of the nutrients. A value closer to 1 corresponds to a higher nutrient quality. Therefore, the algorithm aims to identify the location of a nutritious source with the highest and best-quality nectar, seeking to find a point in the search space that minimizes or maximizes the value of the problem.

In the initial stage of the algorithm, scout bees generate random initial nutrient sources x_{ij} for each parameter using Equation (1), which incorporates the lower and upper limit values.

$$x_{ij} = x_j^{min} + rand(0,1)(x_j^{max} - x_j^{min}) \quad (1)$$

Where,

$$i = 1, 2, \dots, SN$$

$$j = 1, 2, \dots, D$$

The variables i and j represent the indices for the population of bees (SN) and the optimization parameters (D), respectively. The function $rand(0,1)$ generates random values from 0 to 1. The values of x_{max} and x_{min} denote the maximum and minimum limits for parameter j . A boundary control parameter is employed when any source of the nutrient source reaches completion. Typically, the algorithm completion criterion involves a predetermined maximum number of iterations. Research bees search for new nectar sources within their designated area. If the quality of a new source surpasses that of the old source, the information pertaining to the old source is discarded, and the location of the new source is stored.

During the process of identifying a new food source, research bees utilize Equation (2).

$$v_{ij} = x_{ij} + \phi_{ij}(x_{ij} - x_{kj}) \quad (2)$$

Wherein a new source x_i is generated for each food source by introducing random changes to chosen parameters j within the range $[1, D]$. Here, D represents the problem variable, which is defined as a number in the range $\phi_{ij} [-1, 1]$. Subsequently, the quality of the newly generated source is assessed using the equation (3) to determine its fitness value.

$$\text{fitness value } (f_i) = \begin{cases} \frac{1}{1+f_i} & f_i \geq 0 \\ 1 + abs(f_i) & f_i < 0 \end{cases} \quad (3)$$

f_i represents the target function that assesses the significance of neighbouring source decisions. During the selection process between an existing nectar source and an adjacent one, a greedy approach is employed based on their respective suitability values. If the quality of the neighbouring source is seemed better than the current food source x_i , it replaces x_i with the new source V_i , and the progress counter for this resource is reset to zero. Otherwise, if the current resource is retained, the progress counter is incremented by one.

$$p_i = \frac{\text{fitness}_i}{\sum_{i=1}^{SN} \text{fitness}_i}$$

The variable p_i represents the probability value of solution i , while fitness denotes the suitability value of the i^{th} solution. When a specific progress counter for a food source surpasses a predefined threshold limit, the corresponding food source is considered established. At this stage, the research bees accountable for that source transform into scout bees and create a new nutrient source randomly, following the expression given in Eq. (1), as a replacement for the exhausted source. The algorithm continues executing either until reaching the maximum number of iterations or fulfilling certain completion criteria before these steps take place.

3. RESULTS AND DISCUSSION

3.1. Effect of Nano SiC on Mechanical Properties

The tensile, compressive and flexural tests were conducted on the prepared specimens adopting suitable ASTM standards and the results were plotted in the Figure 5. The test results revealed that incorporating SiC nanopowder into the composition of epoxy resin reinforced with basalt and glass fibers led to an enhancement in the tensile properties of the samples. The addition of filler particles served as a stress transfer barrier, resulting in improved tensile strength. Furthermore, the samples indicated an improvement in compressive strength from 170.74 MPa to 327.69 MPa with the addition of nano SiC filler. The substantial improvement in compressive strength was primarily attributed to the strong interfacial bonding between the nano SiC filler and the fiber. Additionally, the flexural strength of the samples filled with nano SiC filler exhibited an increase of approximately 72%. The increase in contact area between the fiber and resin is a key factor in improving the flexural strength of a composite [27]. The experimental observations indicate that when the specimen is positioned on two support

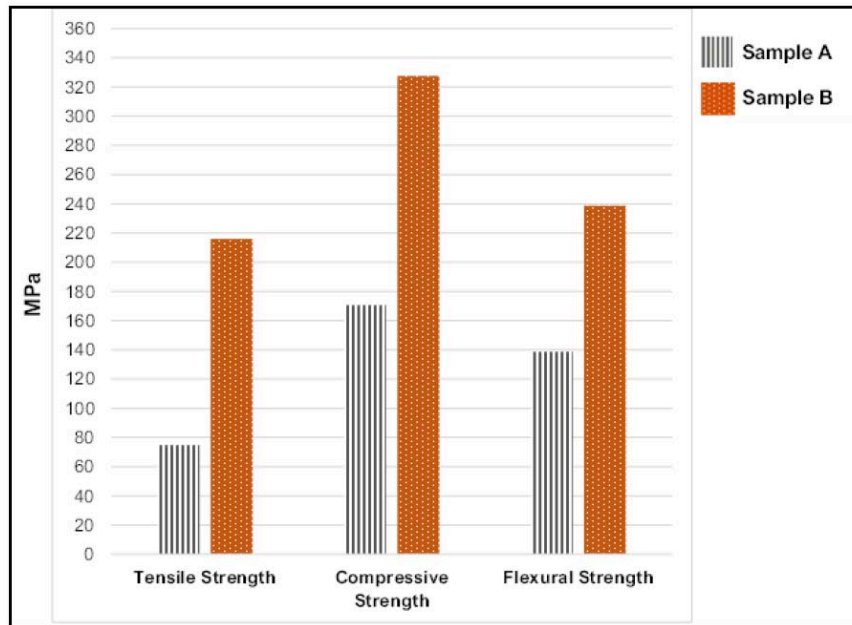


Figure 5: Mechanical Properties of the prepared samples.

points and subjected to a load from the top, it undergoes bending. This bending causes the top layer of the specimen to experience compressive loading, while the bottom layer experiences tensile loading. The presence of a strong bond between the fiber and filler contributes to the increase in flexural strength. This strong bond facilitates the efficient transfer of loads from one end of the specimen to the other, leading to an overall improvement in flexural strength [28].

Figure 6 indicates the impact properties of sample A (basalt-glass polymer composite) and sample B (Nano SiC filled basalt-glass polymer composite). From the figure it is evident that the inclusion of Nano SiC powder as filler in the composite improves the impact properties up to 74%. The observed enhancement in impact strength can be attributed to the presence of a weaker bond within the composite. As the bond strength between the fibers, SiC filler, and the epoxy resin

decreases, the composite's capacity to absorb impact energy increases. Additionally, a significant amount of energy is absorbed through the initiation of cracks along the interface between the fibers, filler, and matrix during the debonding process. The energy absorption capability of composites is influenced by the properties of their constituent materials [28].

3.2. Effect of Process Parameters on AWJM

Through an investigation of the cutting process of clear Plexiglas using an abrasive water jet, the impact of process parameters on the AWJM technique has been examined. This study has revealed two distinct mechanisms responsible for material removal. The first mechanism predominantly operates at the uppermost section of the kerf, characterized by a shallow abrasive impact angle. Here, erosion is the primary mechanism by which material is removed. As the kerf deepens, the abrasive impact angle becomes larger, leading to the dominance of deformation wear as the primary material removal mechanism [29]. The precise mechanics underlying these mechanisms are not yet fully comprehended. However, the ability of AWJM to effectively penetrate thick materials may be attributed to the entrapment of abrasive particles within the jet following the initial impacts at the top of the cut.

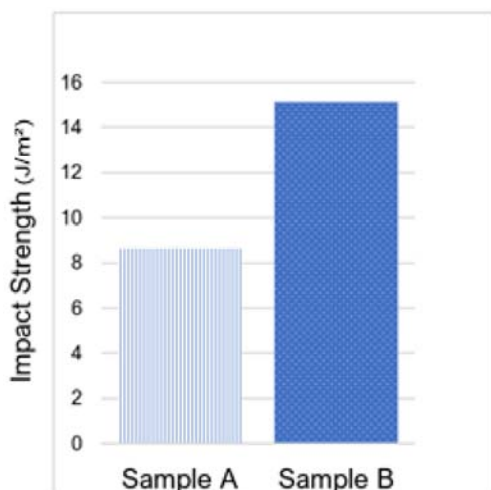


Figure 6: Impact Strength of prepared samples.

The surface roughness of a cut is influenced by the pressure of the water jet used. When the water pressure is higher, it leads to a reduction in the Kerf taper angle and striation angle of the cut, especially when combined with a lower traverse rate during the cutting process [30]. Increasing the water jet pressure results in a higher kinetic energy of the abrasive particles, which maximizes the removal of material

from the surface [31]. As a result, the markings on the machined surface are minimized, leading to a flat finish and a decrease in surface roughness.

Increasing the kinetic energy of the water jet in the Abrasive Water Jet Machining (AWJM) process can lead to enhanced dispersion capability [32]. Optimal machining parameters are suggested to achieve the highest kinetic energy of the water jet, ensuring improved dissemination. When it comes to the type of abrasive material, the hardness of the abrasive has a significant impact on the rupture behavior of the particles. Harder materials, such as SiC, have a higher likelihood of particle fractures, resulting in reduced surface roughness. Similarly, higher hydraulic pressure increases the kinetic energy of the abrasive particles and enhances their material removal capability [33]. Consequently, this leads to a decrease in surface roughness.

The standoff distance in Abrasive Water Jet Machining (AWJM) plays a crucial role in the cutting process. Typically, a higher standoff distance allows the water jet to expand before entering the cutting area, making it more susceptible to the surrounding environment external forces. Consequently, increasing the standoff distance results in a larger jet diameter when cutting is started, leading to a decrease in the kinetic energy density of the jet upon striking the material [34]. On the other hand, maintaining a lower standoff distance can contribute to a smoother surface owing to improved kinetic energy. Therefore, selecting an appropriate standoff distance is essential to achieve the desired surface finish.

Increasing the traverse rate in abrasive water jet cutting leads to a reduction in the machining action overlap and fewer abrasive particles striking the material. This, in turn, results in an increased surface

roughness. Numerous researchers have confirmed that a lower traverse rate is necessary to achieve a better surface finish [16, 35, 36]. The geometry of the kerf is a key consideration in AWJM. It typically exhibits a wider entry and narrows as the jet cuts into the material, forming the kerf. After completing a cut, an abrasive water jet tends to produce a tapered slot, where the top is wider than the bottom. Generally, the taper increases with higher standoff distances and traverse rates, while it decreases with increased pressure. These findings indicate that the taper decreases as the kinetic energy of the abrasive water jet increases [37]. Moreover, it is evident that a lower taper ratio is produced by the abrasive particles with higher hardness.

3.3. SEM Analysis

The surface integrity of glass-basalt fiber reinforced composites was examined to assess the effects on the machined surface, as depicted in Figure 7. SEM images were obtained using a ZEISS machine. The analysis revealed the presence of crack propagation on the machined surface, as shown in Figure 7c. This could be attributed to varying levels of interfacial bonding between the Nano SiC particles and the matrix materials [38]. Figure 7a indicated the occurrence of voids in certain areas of the machined surfaces, likely caused by the existence of dampness in the SiC particles. Subsequently, these voids contributed to crack formation within the composites when pressure was applied in the machining process. Additionally, abrasive impressions observed in specific regions and clusters of fillers were noticed from Figure 7e.

During the machining process, the application of flexural load led to the observation of fiber pull-out, breakage, and bending, contributing to a rougher surface [39]. When the water jet is incapable to cut through the hard fiber-reinforced components within

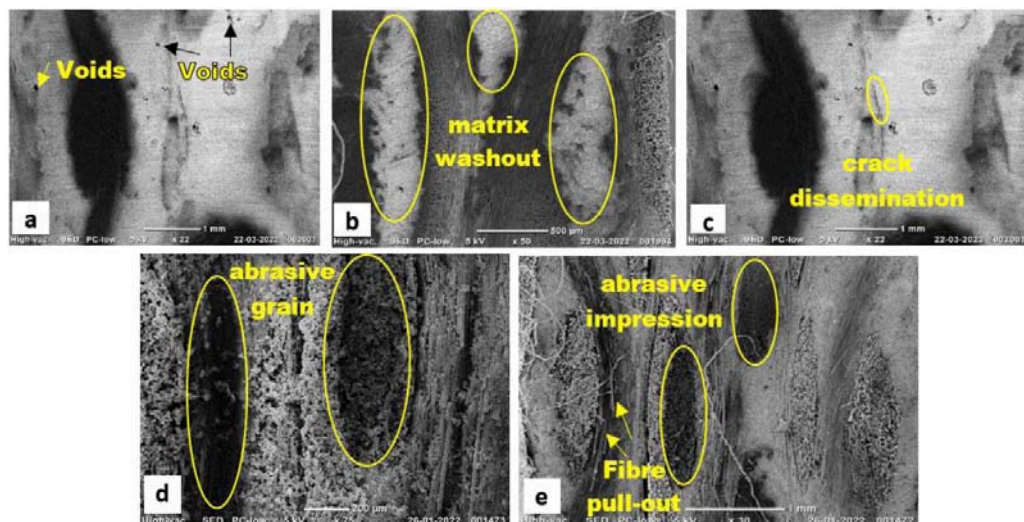


Figure 7: SEM of AWJM sample surfaces.

the matrix, it rebounds and erodes the softer matrix material [40]. This phenomenon results in the noticeable appearance of matrix washout and bulging fibers, as evident in Figure 7b. Figure 7d highlights certain changes, such as clustered SiC particles and abrasive grain marks distributed on the machined surfaces. This confirms that the MRR is influenced by the interaction of abrasive particles with water pressure [41]. In some areas, the presence of hole patches indicates the destruction of ceramic materials due to abrasive particles with sharp corners. This effect is particularly prominent when using a higher standoff distance (A) and a lower cutting speed (C) [42].

3.4. Optimization of Process Parameter using Swarm Intelligence Algorithm

The swarm intelligence algorithm is included with the required changes to suit defined non-linear optimistic tasks with unique design variables. A case with restrictions on the main point solution of the limited optimization process. The main point in the process of defined optimization is to work with constraints related to solution variables. In current work, the limits are effectively processed by maintaining the feasibility of developed solutions [43]. To limit the optimal solution to the possible space, each artificial bee is forced to search. To control the optimal solution to the possible place, every artificial bee is done to search for the whole solution, but only when it develops, as it grows. In addition, this process is accelerated by initiating artificial bees in the variable solution [44]. The variables of the project associated with the current optimization problem are discrete in nature. The swarm intelligence algorithm used in the current work is changed as per boundary conditions to processing discrete variables. There are two essential variables which consider material removal rate (MRR) and surface roughness (SR) corresponding to four input parameters (Stand-off distance, Jet pressure, Speed and two samples (Basalt/0% nano SiC, Basalt/1% nano SiC) is capable to taking within the limits of the specified range doing their discrete in nature. This practice was adopted taking into account the preservation of the practicality of the developed solution on the basis of its productivity [45].

To demonstrate the effectiveness of the Swarm Intelligence algorithm in optimizing parameters, this study focuses on the properties of AWJM. Specifically, a multi-objective optimization is conducted for the AWJ cutting process, considering four key process parameters. The primary aim of this investigation is to simultaneously maximize metal removal rate (MRR) and minimize surface roughness (SR). Thus, the objective can be formulated as follows:

$$\text{Maximize (MRR)} = f(JP, SOD, N, Sp)$$

$$\text{Minimize (SR)} = f(JP, SOD, N, Sp)$$

In order to validate and showcase the effectiveness of the RSM-based Artificial Bee Colony algorithm in optimizing parameters for abrasive water jet machining, the following multi-objective optimization model is formulated:

Sample A

$$\begin{aligned} SR_{Ra} = & +1.38647 - 2.10026e^{-4} \times A \times 0.027341 \times B \\ & + 0.029636 \times C - 2.6341e^{-5} \times AB \\ & + 5.28315e^{-5} \times AC - 1.71806e^{-3} \times BC \\ & + 2.84747e^{-7} \times A^2 \\ & - 5.92356e^{-4} \times B^2 \times 3.05001e^{-3} \times C^2 \end{aligned}$$

$$\begin{aligned} MRR_{m^3/Sec} = & -0.19725 \\ & - 6.57926e^{-4} \times A \times 3.60239e^{-3} \times B \\ & + 0.090846 \times C - 3.32436e^{-5} \times AB \\ & + 1.57596e^{-5} \times AC - 3.24080e^{-4} \times BC \\ & + 1.08205e^{-7} \times A^2 \\ & - 8.01966e^{-4} \times B^2 \times 1.16433e^{-3} \times C^2 \end{aligned}$$

Sample B

$$\begin{aligned} SR_{Ra} = & +1.36715 - 3.11463e^{-4} \times A \times 0.034251 \times B \\ & + 0.010845 \times C - 2.63415e^{-5} \times AB \\ & + 5.28315e^{-5} \times AC - 1.71806e^{-3} \times BC \\ & + 2.84747e^{-7} \times A^2 \\ & - 5.92356e^{-4} \times B^2 \times 3.0500e^{-3} \times C^2 \end{aligned}$$

$$\begin{aligned} MRR_{m^3/Sec} = & -0.15531 \\ & + 6.33357e^{-4} \times A \times 4.42280e^{-3} \times B \\ & + 0.097741 \times C - 3.32436e^{-5} \times AB \\ & + 1.57596e^{-5} \times AC - 3.24080e^{-3} \times BC \\ & + 1.08205e^{-7} \times A^2 \\ & - 8.01966e^{-4} \times B^2 \times 1.16433e^{-3} \times C^2 \end{aligned}$$

This study deals with multi objective optimization issues, so it is a practical method of solutions that convert this multi-scale problem into a single-scale problem. Therefore, the following objective functions as mentioned in equation (4), including all quality characteristics, are used for all purposes.

$$\text{MOO (z)} = w_1 \times \overline{MRR} - w_2 \times \overline{SR} \tag{4}$$

Where, w_1 and w_2 as assumed was equal importance to 0.5 in this investigation. Metal Removal Rate (\overline{MRR}) and Surface Roughness (\overline{SR}) are the normalized values of MRR and SR which are obtained by the following equations (5) and (6),

$$\overline{MRR} = \frac{MRR_{Max} - MRR}{SR_{max} - SR_{min}} \tag{5}$$

$$\overline{SR} = \frac{SR - SR_{min}}{SR_{max} - SR_{min}} \tag{6}$$

The term “min” and “max” indicated minimum and maximum characteristics of the responses obtained from the experimentation. And the term indicated without any index is representing the value received from RSM. The following are the boundary conditions considered for the analysis and for the development of empirical model as per the available data range produced by the design matrix. The constraints are,

- Jet pressure (X_1) = 200 MPa – 600 MPa
- Stand-off distance (X_2) = 3mm – 15mm
- Speed (X_3) = 2mm/min – 10mm/min

In the equation, the quality characteristics that need to be increased are characterized by negative signs. This is because the Swarm intelligence algorithm is designed and created for the purpose of minimization mechanism. Therefore, quoting the negative sign allows to deal with this problem. The developed multi-objective function is associated with the Swarm intelligence algorithm and is optimized using the following formula for each sample (A) and sample (B) is given below,

Sample A

$$MOO_{(SR+MRR)} = 0.730 + 5.17e^{-3} \times A + 0.014 \times B + 0.11 \times C - 5.086e^{-5} \times AB + 5.109e^{-5} \times AC - 8.25e^{-3} \times BC + 8.226e^{-8} \times A^2 + 4.05e^{-2} \times B^2 + 8.75e^{-2} \times C^2$$

Sample B

$$MOO_{(SR+MRR)} = 0.272 + 2.23e^{-4} \times A + 0.00656 \times B + 0.0493 \times C - 2.256e^{-5} \times AC + 2.80e^{-4} \times BC + 2.056e^{-8} \times A^2 + 2.32e^{-4} \times B^2 + 2.17e^{-4} \times C^2$$

The parameters used for the optimization is given below,

- No of food sources = 20
- No of onlooker bees = 50
- No of scout bees = 1
- Maximum iteration = 300

The program to optimize AWJ, subjecting parameters of the control to machining which will lead to minimal value Ra and to maximize metal removal rate (MRR), has been developed and carried out use of software MATLAB (R2010A). During the experiment, three control parameters of the Swarm Intelligence algorithm were employed. The number of bees in the colony was regulated to limit the attempts made to improve each food source. Thereafter the control parameters set as,

- 200 MPa < X_1 < 600 MPa
- 3mm < X_2 < 15mm
- 2mm/min < X_3 < 10mm/min

Table 6: Optimum Cutting Parameters

Sample	Jet Pressure (MPa)	Stand-off distance (mm)	Speed (mm/min)	Surface roughness (Ra) μ m	Metal removal rate (MRR) mm ³ /sec
A	552.2961	5.7777	9.7560	1.568	0.823
B	561.8018	4.5488	9.9437	1.645	0.918

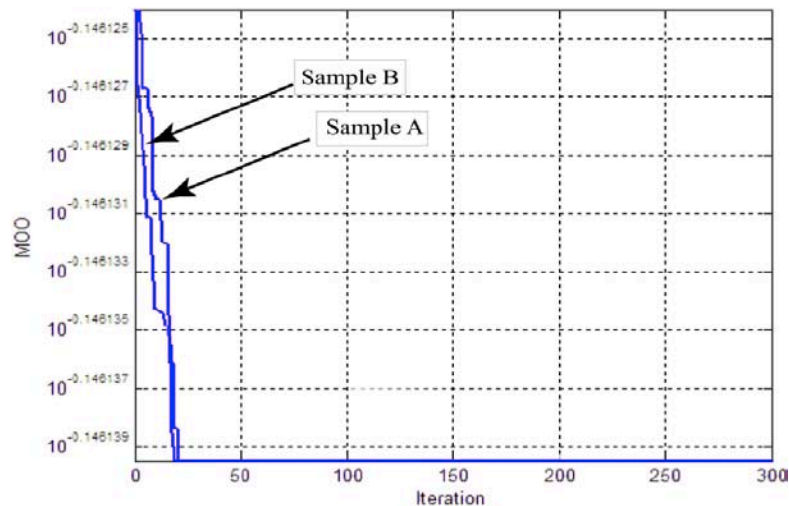


Figure 8: Convergence Plot for Sample A and Sample B.

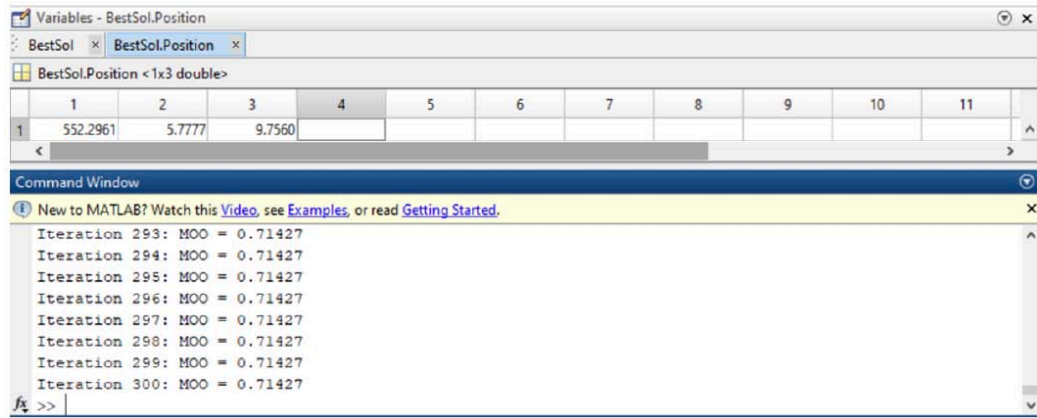


Figure 9: Convergence Value for Sample A.

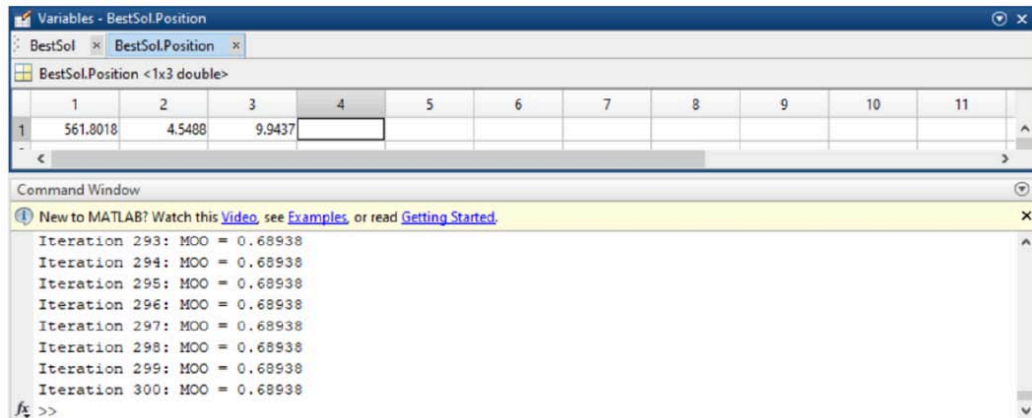


Figure 10: Convergence Value for Sample B.

The algorithm is checked up on the standard metrics of work, percentage success, the best, the worst, average, and average scores. The optimal cutting parameters obtained from the algorithm are speed, stand-off distance and Jet pressure for each sample A and sample B are presented in Table 6 and convergence plot is presented in Figure 8 also the convergence values are obtained from Figures 9 and 10. The results showed that the Swarm intelligence algorithm reduced mean surface roughness (Ra) and increased metal removal rate (MRR) for all 24 experimental runs. The optimal value obtained through the Swarm Intelligence algorithm aligns well with the solution and experimental outcomes estimated by the response surface method. This indicates that the Swarm Intelligence algorithm is stable and consistently produces high-quality solutions.

4. CONCLUSION

The present study focuses on analyzing the performance of Abrasive Water Jet Machining (AWJM) on a hybrid basalt-glass fiber reinforced epoxy composite filled with nano SiC particles. The analysis includes evaluating the surface roughness (Ra) and Material Removal Rate (MRR) using the Swarm Intelligence algorithm.

- To attain improved surface finish and Material Removal Rate (MRR), an optimal combination of Abrasive Water Jet (AWJ) cutting parameters was determined. The optimum levels of the input process parameters were identified as follows: a cutting speed of 9.75 mm/min., a stand-off distance of 5.78mm, and a jet pressure of 553 MPa.
- The water jet pressure directly affects the surface roughness of the cut. Increasing the water jet pressure maximizes the kinetic energy of the abrasive particles. Additionally, the surface roughness decreases substantially using harder SiC material
- It has been established that maintaining a lower standoff distance results in a smoother surface owing to the enhanced kinetic energy. Similarly, increasing the traverse rate leads to a decrease in the machining action overlap and fewer abrasive particles impinging on the surface, thereby increasing the surface roughness.
- SEM analysis of the machined surface indicates the presence of voids, abrasive impressions and clusters of fillers. Additionally, the observation of fiber pull-out, breakage, and bending during

machining, caused by flexural load, contributes to a rougher surface.

REFERENCES

- [1] Li Z, Ma J, Ma H, Xu X. Properties and Applications of Basalt Fiber and Its Composites. *IOP Conf Ser: Earth Environ Sci* 2018; 186: 012052. <https://doi.org/10.1088/1755-1315/186/2/012052>
- [2] Jain A, Singh B, Sharma KK, Shrivastava Y. Fabrication, Testing and Machining of Hybrid Basalt-Glass Fiber Reinforced Plastic composite. *Indian J Pure Appl Phys* 2021; 59: 258-262.
- [3] Santos MD, De Oliveira LA, Bueno AHS, Da Silva LJ, Del Pino GG, Panzera TH. Effect of Ageing on the Mechanical Performance of Thermoset Polymers: A Statistical Approach. *J Res Updates Polym Sci* 2020; 9: 42-29. <https://doi.org/10.6000/1929-5995.2020.09.04>
- [4] Cheloni JPM, Silveira ME, Najar Lopes ES, Da Silva LJ. Fatigue and Failure Analysis of Sandwich Composites using Two Types of Cross-Ply Glass Fibers Laminates and Epoxy Resin. *J Res Updates Polym Sci* 2022; 11: 36-44. <https://doi.org/10.6000/1929-5995.2022.11.06>
- [5] Bandeira CF, Montoro SR, Faria ST, Moreira PRS, Pereira ACC, Oliveira LF, Milanese AC. Degradability of Epoxy/Sisal Fiber Composites via Simulated Soil. *J Res Updates Polym Sci* 2017; 6: 12-16. <https://doi.org/10.6000/1929-5995.2017.06.01.2>
- [6] Yuvaraj N, Pradeep Kumar M, Mugilvalavan M, Shakeel Ahmed LAK. Abrasive Water Jet Machining process: A state of art of review. *J Manuf Process* 2020; 49: 271-322. <https://doi.org/10.1016/j.jmapro.2019.11.030>
- [7] Momber AW, Kovacevic R. Principles of abrasive water jet machining. First ed. Springer-Verlag London Limited, London 1998. <https://doi.org/10.1007/978-1-4471-1572-4>
- [8] Thirumalai Kumaran S, Uthayakumar M, Mathiyazhagan P, Krishna Kumar K, Muthu Kumar P. Effect of abrasive grain size of the AWJM performance on AA (6351)-SiC-B4C hybrid composite. *Appl Mech Mater* 2015. <https://doi.org/10.4028/www.scientific.net/AMM.766-767.324>
- [9] Bitter JG. A study of erosion phenomena part I. *Wear* 1963a; 6(1): 5-21. [https://doi.org/10.1016/0043-1648\(63\)90003-6](https://doi.org/10.1016/0043-1648(63)90003-6)
- [10] Bitter JG. A study of erosion phenomena part II. *Wear* 1963b; 6(3): 169-190. [https://doi.org/10.1016/0043-1648\(63\)90073-5](https://doi.org/10.1016/0043-1648(63)90073-5)
- [11] Sheldon GL, Finnie I. The mechanism of material removal in the erosive cutting of brittle materials. *J Eng Ind* 1966; 88(4): 393-399. <https://doi.org/10.1115/1.3672667>
- [12] Niranjana CA, Srinivas S, Ramachandra M. Effect of process parameters on depth of penetration and topography of AZ91 magnesium alloy in abrasive water jet cutting. *J Magnes Alloy* 2018; 6: 366-374. <https://doi.org/10.1016/j.jma.2018.07.001>
- [13] Hlaváč LM. Investigation of the abrasive water jet trajectory curvature inside the kerf. *J Mater Process Technol* 2009; 209(8): 4154-4161. <https://doi.org/10.1016/j.jmatprotec.2008.10.009>
- [14] Srinivas S, Babu NR. Role of garnet and silicon carbide abrasives in abrasive waterjet cutting of aluminum-silicon carbide particulate metal matrix composites. *Int J Appl Mech* 2011; 1: 109-122. <https://doi.org/10.47893/IJARME.2011.1022>
- [15] Wang J, Wong WCK. A study of abrasive waterjet cutting of metallic coated sheet steels. *Int J Mach Tools Manuf* 1999; 39(6): 855-870. [https://doi.org/10.1016/S0890-6955\(98\)00078-9](https://doi.org/10.1016/S0890-6955(98)00078-9)
- [16] Azmir MA, Ahsan AK, Rahmah A. Effect of abrasive water jet machining parameters on aramid fibre reinforced plastics composite. *Int J Mater Form* 2009; 2(1): 37-44. <https://doi.org/10.1007/s12289-008-0388-2>
- [17] muthak kannan P, Manikandan V, Uthayakumar M, Arun Prasath K, Sureshkumar S. Investigation of the Machining Performance of Basalt Fiber Composites by Abrasive Water Jet Machining. *Mater Phys Mech* 2021; 47: 830-842.
- [18] Samanta S, Chakraborty S. Parametric optimization of some non-traditional machining processes using artificial bee colony algorithm. *Eng Appl Artif Intell* 2011; 24(6): 946-957. <https://doi.org/10.1016/j.engappai.2011.03.009>
- [19] Yusup N, Sarkheyli A, Zain AM, Hashim SZM, Ithnin N. Estimation of optimal machining control parameters using artificial bee colony. *J Intell Manuf* 2014; 25(6): 1463-1472. <https://doi.org/10.1007/s10845-013-0753-y>
- [20] Yusup N, Zain AM, Hashim SZM. Evolutionary techniques in optimizing machining parameters: Review and recent applications (2007–2011). *Expert Syst Appl* 2012; 39(10): 9909-9927. <https://doi.org/10.1016/j.eswa.2012.02.109>
- [21] Mohan K, Rajmohan T. Fabrication and Characterization of MWCNT Filled Hybrid Natural Fiber Composites. *J Nat Fibers* 2017; 14(6): 864-874. <https://doi.org/10.1080/15440478.2017.1300115>
- [22] Adem AM, Azmeraw HE. The manufacturing practices and parameters optimization on abrasive jet machining for surface preparation of mild steels. *Results Eng* 2022; 15: 100457. <https://doi.org/10.1016/j.rineng.2022.100457>
- [23] Karaboga D, Basturk B. On the performance of artificial bee colony (ABC) algorithm. *Appl Soft Comput* 2008; 8(1): 687-697. <https://doi.org/10.1016/j.asoc.2007.05.007>
- [24] Vijayan D, Rajmohan T. Modeling and evolutionary computation on drilling of carbon fiber-reinforced polymer nanocomposite: an integrated approach using RSM based PSO. *J Braz Soc Mech Sci Eng* 2019; 41: 395. <https://doi.org/10.1007/s40430-019-1892-7>
- [25] Nandakumar A, Rajmohan T, Vijayabhaskar S, Vijayan D. Sustainable Grinding Performances of Nano-Sic Reinforced Al Matrix Composites under MQL: An Integrated Box- Behnken Design Coupled with Artificial Bee Colony (ABC) Algorithm. *Sustain Chem* 2022; 3(4): 482-510. <https://doi.org/10.3390/suschem3040030>
- [26] Jahjouh MM, Arafa MH, Alqedra MA. Artificial Bee Colony (ABC) algorithm in the design optimization of RC continuous beams. *Struct Multidiscip Optim* 2013; 47(6): 963-979. <https://doi.org/10.1007/s00158-013-0884-y>
- [27] He H, Li K. Study on Flexural Strength and Flexural Failure Modes of Carbon Fiber/Epoxy Resin Composites. *J Res Updates Polym Sci* 2014; 3: 10-15. <https://doi.org/10.6000/1929-5995.2014.03.01.2>
- [28] Agarwal G, Patnaik A, Sharma RK. Thermo-mechanical properties of silicon carbide filled chopped glass fiber reinforced epoxy composites. *Int J Adv Struct Eng* 2013; 5(1): 1-8. <https://doi.org/10.1186/2008-6695-5-21>
- [29] Gnanavelbabu A, Rajkumar K, Saravanan P. Investigation on the cutting quality characteristics of abrasive water jet machining of AA6061-B4C-hBN hybrid metal matrix composites. *Mater Manuf Process* 2018; 33(12): 1313-23. <https://doi.org/10.1080/10426914.2018.1453146>
- [30] Kumar KR, Sreebalaji VS, Pridhar T. Characterization and optimization of abrasive water jet machining parameters of aluminium/tungsten carbide composites. *Measurement* 2018; 117: 57-66. <https://doi.org/10.1016/j.measurement.2017.11.059>
- [31] Khan AA, Munajat NB, Tajudin HB. A study on abrasive water jet machining of aluminum with garnet abrasives. *Int J Appl Sci* 2005; 5(9): 1650-1654. <https://doi.org/10.3923/jas.2005.1650.1654>
- [32] Llanto JM, Vafadar A, Aamir M, Tolouei-Rad M. Analysis and Optimization of Process Parameters in Abrasive Waterjet Contour Cutting of AISI 304L. *Metals* 2021; 11: 1362. <https://doi.org/10.3390/met11091362>

- [33] Azmir MA, Ahsan AK. A study of abrasive water jet machining process on glass/ epoxy composite laminate. *J Mater Process Technol* 2009; 209(20): 6168-6173. <https://doi.org/10.1016/j.jmatprotec.2009.08.011>
- [34] Azmir MA, Ahsan AK. Investigation on glass/epoxy composite surfaces machined by abrasive water jet machining. *J Mater Process Technol* 2008; 198(1-3): 122-128. <https://doi.org/10.1016/j.jmatprotec.2007.07.014>
- [35] Chithirai Pon Selvan M, Mohana Sundara Raju N, Sachidananda HK. Effects of process parameters on surface roughness in abrasive waterjet cutting of aluminium. *Front Mech Eng* 2012; 7(4): 439-444. <https://doi.org/10.1007/s11465-012-0337-0>
- [36] Begic-Hajdarevic D, Cekic A, Mehmedovic M, Djelmic A. Experimental study on surface roughness in abrasive water jet cutting. *Procedia Eng* 2015; 100: 394-399. <https://doi.org/10.1016/j.proeng.2015.01.383>
- [37] Wong IMM, Azmi AI, Lee CC, Mansor AF. Kerf taper and delamination damage minimization of FRP hybrid composites under abrasive water-jet machining. *Int J Adv Manuf Technol* 2018; 94(5): 1727-1744. <https://doi.org/10.1007/s00170-016-9669-y>
- [38] Teng X, Chen W, Huo D, Shyha I, Lin C. Comparison of cutting mechanism when machining micro and nano-particles reinforced SiC/Al metal matrix composites. *Compos Struct* 2018; 203: 636-647. <https://doi.org/10.1016/j.compstruct.2018.07.076>
- [39] Yan L, Chou N, Huang L, Kasal, B. Effect of alkali treatment on microstructure and mechanical properties of coir fibres, coir fibre reinforced-polymer composites and reinforced-cementitious composites. *Constr Build Mater* 2016; 112: 168-182. <https://doi.org/10.1016/j.conbuildmat.2016.02.182>
- [40] Zhao Y, Lu W, Zhu Y, Zuo D. Pretreatment of aircraft carbon fiber-reinforced plastic skin by plastic abrasive jet machining. *J Adhes Sci Technol* 2022: 1-23. <https://doi.org/10.1080/01694243.2022.2128302>
- [41] Kumar UA, Alam SM, Laxminarayana P. Influence of abrasive water jet cutting on glass fibre reinforced polymer (GFRP) composites. *Mater Today: Proc* 2020; 27: 1651-1654. <https://doi.org/10.1016/j.matpr.2020.03.554>
- [42] Rakshit R, Das AK. A review on cutting of industrial ceramic materials. *Precis Eng* 2019; 59: 90-109. <https://doi.org/10.1016/j.precisioneng.2019.05.009>
- [43] Prasanth RSS, Hans Raj K. Optimization of straight cylindrical turning using artificial bee colony (ABC) algorithm. *J Inst Eng (India)* 2017C; 98(2): 171-177. <https://doi.org/10.1007/s40032-016-0263-8>
- [44] Salehi M, Hosseinzadeh M, Elyasi M. A study on optimal design of process parameters in tube drawing process of rectangular parts by combining box-behnken design of experiment, response surface methodology and artificial bee colony algorithm. *Trans Indian Inst Met* 2016; 69(6): 1223-1235. <https://doi.org/10.1007/s12666-015-0670-1>
- [45] Vijayan D, Rajmohan T. Influence of Fiber Content on Tensile and Flexural Properties of Ramie/Areca Fiber Composite—An Algorithmic Approach Using Firefly Algorithm, in: Palanikumar K, Thiagarajan R, Latha B. (Eds.) *Bio-Fiber Reinforced Composite Materials*. Composites Science and Technology. Springer, Singapore 2022; pp. 235-252. https://doi.org/10.1007/978-981-16-8899-7_14

Received on 06-08-2023

Accepted on 02-09-2023

Published on 25-09-2023

<https://doi.org/10.6000/1929-5995.2023.12.11>© 2023 Vijayabhaskar *et al.*; Licensee Lifescience Global.

This is an open-access article licensed under the terms of the Creative Commons Attribution License (<http://creativecommons.org/licenses/by/4.0/>), which permits unrestricted use, distribution, and reproduction in any medium, provided the work is properly cited.